Recovering Orientation of a textured planar surface using wavelet transform

Thomas Greiner
School of Engineering, University of Applied Sciences
Tiefenbronner Str. 65, D-75175 Pforzheim, Germany.
Email: Tgreiner@fh-pforzheim.de

Sukhendu Das
School of Engineering, University of Applied Sciences
Tiefenbronner Str. 65, D-75175 Pforzheim, Germany.
Email: sdas@fh-pforzheim.de

Abstract: Shape from texture has received a great deal of attention in the past few decades. This paper analyzes the spectral variations of texture spatial frequencies as a function of orientation and depth of a 3-D planar surface. Based on this relationship we attempt to derive an expression for the extraction of 3-D surface orientation using texture features alone. Using experimentation on simulated texture images, we illustrate the advantage of using 1-D wavelets for this purpose.

Key Words: Texture, orientation, wavelet, spectral energy, separable analysis, variance

1. Introduction

In the field of computer vision and pattern recognition, the problem of extracting 3-D surface orientation from a monocular texture image has received a great deal of attention [1-3, 6, 7, 10, 11, 14-16, 18, 19]. If the surface exhibits a textured pattern, it is often easy for a human being to extract the structure information from the image. But the problem is ill-posed for a machine to solve. This paper presents analytical expressions using separable 1-D analysis of 2-D images for extraction of surface orientation of a textured planar surface.

In this paper we use a model of the viewing geometry which is similar to that used by Nayar et. al. [4, 12, 13] in Curet database {www.cs.columbia.edu/CAVE/curet}, but different from the one used by Super and Bovik [18-19], Ribeiro and Hancock [14] and Leung and Malik [11]. Dana and Nayar [4, 12] however proposed this model of the viewing geometry for measurements of surface reflectance of textured surfaces, based of different viewing angles and illumination. A few others [8, 17] have proposed visualization of surfaces using 3-D textures. The work by Malik [11] used density, height and occlusion to derive the shape from textures. Bovik [18], and Hancock [14] in their work have attempted to extract surface orientation using spectral gradient, peaks and distortion. Most of the earlier work [1, 2, 6, 7, 18, 19] involved an exhaustive numerical search. Ribeiro and Hancock [14] uses the eigenstructure of an affine distortion matrix to extract orientation. The most recent work by Clerc and Mallat [3] uses Warplets (affine transformation of the mother wavelets) to recover shape using statistical estimates. Texture is realized as a stochastic process. Deformation gradient is estimated using the 'texture gradient equation' which models the 'Warpogram' (variance of the wavelet coefficients) of the image.

We present a simpler algorithm and analysis based on 1-D wavelets to study the spectral variations in a textured planar surface as a function of its depth and orientation. The advantage with our method will be the separable analysis in both dimensions of the image to extract the individual components of the surface orientation parameters. This will be evident in the next section, when we present the viewing geometry and derive the analytical expressions. Due to separable analysis, errors in computation of one of the orientation angles will not effect the other, which is a drawback in the method suggested in [14]. We then present the need and use of a multi-resolution filter (wavelet) for spectral analysis of texture surfaces to extract the surface orientation.

2. Basic texture projective equations

Figure 1. shows the viewing geometry and coordinate system used. Consider a surface element S, containing a simple sinusoidal texture. This simplicity is assumed to derive the relationship between spectral features of the texture pattern in the image space and 3-D surface parameters (depth and surface orientation) of S.
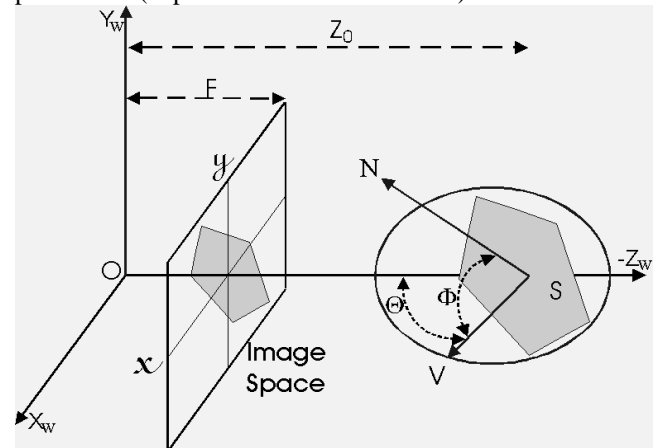

Figure 1. Viewing geometry and coordinate system.

Let N be the surface normal on S. This vector is defined using polar and azimuth angles of N w.r.t the world coordinate system. The azimuth angle ϕ, is the angle between the vector N and its projection, V, on the horizontal Z_W-X_W plane. The polar angle, θ (in the Z_W-X_W plane), is the angle between the vector V and Z_W axis, clock-wise looking along the Y-axis from the origin. This model is similar to that used in the CURET database [4, 12]. The view axis is along the $-Z_W$ axis and F be the focal length of the viewing system, assuming a pin-hole camera configuration and perspective geometry of the viewing setup. The image plane (2-D) coordinate system is aligned with the X_W-Y_W axis of the world-coordinate system.

Assume a simple sinusoidal texture pattern on a planar surface with frequency f_r. Let the surface S be at a distance Z_0, from the origin. Let the surface inclination be such that either θ or ϕ is zero and the other be a non-zero value

α. The advantage of the viewing geometry can be seen here. Local spectral gradient or variations along the x-axis (horizontal direction) of the image plane vanish when θ = 0. Similarly, when φ = 0, the spectral variations of the texture along the y-axis (vertical direction) of the image plane is zero.

When only one of the components of the angles of the surface orientation is non-zero (say, φ), and the other zero, the local spectral variations will be only along one of the principal axis (in this case, y-axis) of the image plane. Let the frequency content of the sinusoidal texture on a planar surface, at a distance Z_0 from the origin and oriented orthogonal to the viewing direction, as observed in the image space be a local spectral peak at f_r. Let f_r be assumed to be known initially (this constraints will be relaxed later on). Assume orthogonal projection initially, without any loss of generality. Perspective projection and effect of depth will be considered and incorporated next. If the surface is inclined such that, θ = 0 and φ = α, then the observed frequency peak will be, $f_r' = f_r \sec(\alpha)$. (1)

This relation is illustrated in figure 2. Eqn. (1) gives the relation between the observed frequency of the texture surface and inclination of the surface w.r.t. viewing direction. Thus if θ = β and φ = α, then the observed frequency will be, $f_r'' = f_r \sec(\beta) . \sec(\alpha)$ (2)
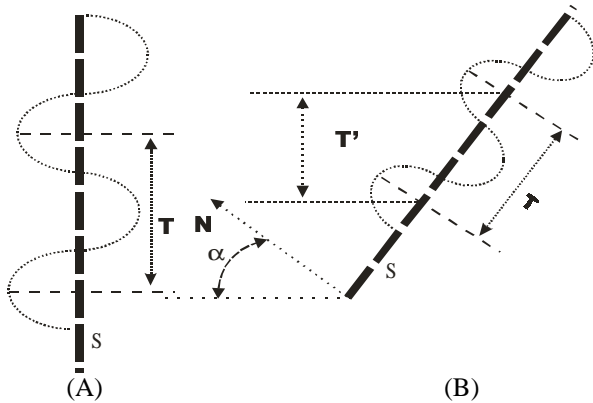
Figure 2. (A) A simple sinusoid texture pattern on a planar surface S, oriented orthogonal to the viewing direction (θ = φ = 0). (B) The surface is oriented at φ = α and θ = 0. The projection of one period of the sinusoid is, T' = T cos(α). Orthogonal projection is assumed and the sinusoidal texture pattern is shown as a dotted curve on the planar surface S.

Let us now observe the effect of depth of the surface from the viewer on the frequency peak. From figure 3(A), we can write using perspective projection models, the following equation:
H/Z₀ = h/F (3)
where H is the time period of the sinusoid on the object surface, and h (= 1/ f_r) is the observed time period on the image plane. If the surface is moved away from the viewer by a distance ΔZ, then
H/Z' = h'/F (4)
where Z' = Z_0 + ΔZ, and h' is the observed time period of the sinusoid under perspective projection. Combining equations (3) and (4), we have:

$$h' = \frac{FH}{Z'} = \frac{FH}{(Z_0 + \Delta Z)} = \frac{FH}{Z_0(1 + \frac{\Delta Z}{Z_0})} = \frac{h}{1 + \frac{\Delta Z}{Z_0}} \quad (5)$$

The observed frequency, f_z, now is:

$$f_z = \frac{1}{h'} = \frac{1 + \frac{\Delta Z}{Z_0}}{h} = f_r(1 + \frac{\Delta Z}{Z_0}) \quad (6)$$
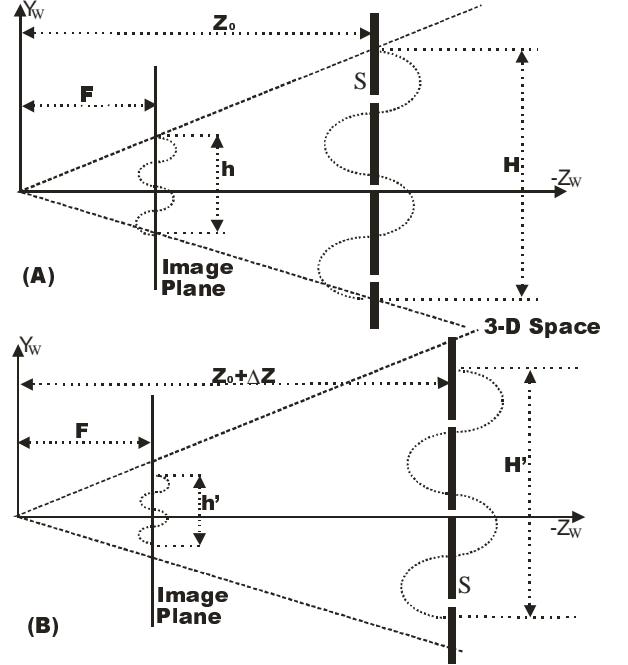
Figure 3. A planar object surface, S, with a simple sinusoidal texture pattern and oriented orthogonal to the viewing direction is projected on the image plane. (A) Surface is at a distance Z_0 from the camera and length of the projected segment is h. (B) Surface is at a distance (Z_0 + ΔZ) from the camera and length of the projected segment is h'. F is the focal length of the camera.

From equations (2) and (6), we get the locally observed frequency f_{oi}, of a planar surface at depth (Z_0 + ΔZ_i), and orientation θ = β, φ = α, as:

$$f_{oi} = f_r(1 + \frac{\Delta Z_i}{Z_0})(\sec\alpha)(\sec\beta)$$
$$= f_r(\frac{Z_i}{Z_0})(\sec\alpha)(\sec\beta) \quad (7)$$

where, $Z_i = Z_0 + \Delta Z_i$.

Equation 7 is the basic equation for the observed texture frequency in the image plane, depending on the surface parameters (depth (Z_0 + ΔZ_i) and orientation α, β). The plot in Figure 4, illustrates the nature of the frequency variation, given in equation (7), as a function of relative depth ($\Delta Z_i/Z_0$) and one of the orientation angles (α or β), where the normalized observed frequency is (f_{oi}/f_r).

If any texture pattern can be considered as a superposition of several sinusoids (band-limited), then all the individual components of the signal will also be effected in a similar manner as in equation (7). We will now derive equations which estimate these parameters from the observed frequency f_{oi}, on the image plane. Henceforth, the term

'frequency' will mean the observed local spectral peak of the texture around a neighborhood of a point in the image plane.

3. Method to estimate orientation parameters

Observe Figure 5, which shows the perspective geometry of a planar surface S with orientation $\phi = \alpha$ and $\theta = 0$. Select two points I and J, on the vertical axis on the image plane, with coordinates (x_i, y_i) and (x_i, y_j) respectively. These may be considered to be the projections on the image plane of points P_i and P_j on S, with depth Z_i and Z_j respectively.
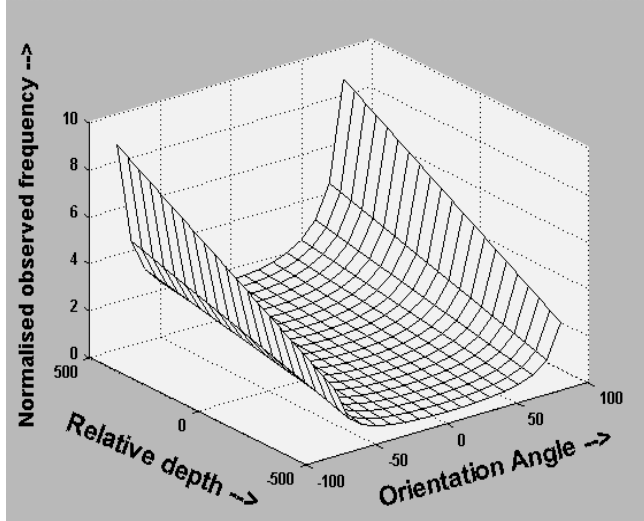

Figure 4. Normalized observed frequency (f_{oi}/f_r), in the image texture pattern, as a function of relative depth ΔZ_i and orientation angle α.

In equation(7), substituting $\phi = \alpha$ and $\theta = 0$ at a point (x_i, y_i) in the image plane, we have:

$$f_{oi} = f_r(1+\frac{\Delta Z_i}{Z_0})(\sec\alpha) \qquad (8)$$

and at a point (x_i, y_j) in the image plane:

$$f_{oj} = f_r(1+\frac{\Delta Z_j}{Z_0})(\sec\alpha) \qquad (9)$$

Since the polar angle $\theta = 0$, the spectral gradient along the horizontal (x) axis of the image is zero. Hence we look for the variations in spectral values along the vertical (y) axis of the image plane. This role is reversed if $\phi = 0$ and $\theta = \beta$. From equations (8) and (9), we can obtain the difference in the observed frequencies as:

$$\Delta f_o^{i,j} = f_{oj} - f_{oi} = f_{rp}\frac{\Delta Z_{ij}}{Z_0} \qquad (10)$$

where, $\Delta Z_{ij} = Z_j - Z_i$ $(= \Delta Z_j - \Delta Z_i)$ and $f_{rp} = f_r (\sec\alpha)$.
Setting $\Delta Z_i = -\Delta Z_j = -\Delta Z_{ij}/2$ $\qquad (11)$
We have, $\Delta Z_{ij} = Z_j - Z_i = \Delta Z_j - \Delta Z_i = 2\Delta Z_j = -2\Delta Z_i$

Let the factor $(\Delta Z_{ij}/Z_0)$ be represented by K. K denotes the relative difference in depth of two points (P_i and P_j) on S, which are equidistant from a reference point P_0 with depth Z_0. A method to identify such a pair of points from the image plane, will be discussed later.

From the constraint given in equation (11), we can write from equations (8) and (9):

$$f_{0i} + f_{0j} = 2f_{rp} \qquad (12)$$

Using equations (10) and (12) we can write:

$$K = \frac{f_{0j} - f_{0i}}{f_{rp}} = 2[\frac{f_{0j} - f_{0i}}{f_{0j} + f_{0i}}]$$

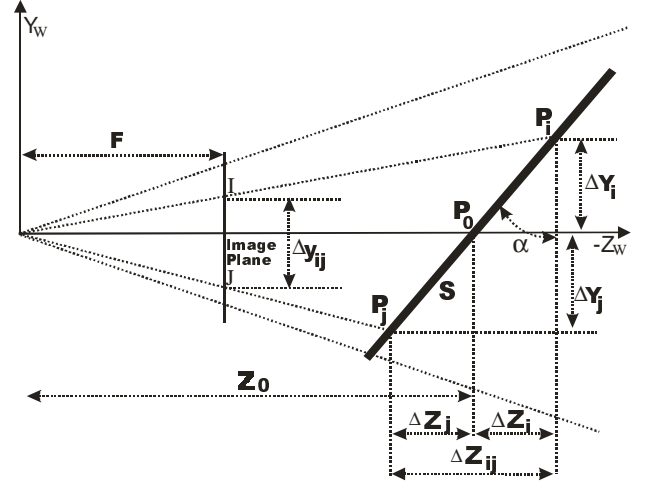$$= 2[\frac{f_d - 1}{f_d + 1}] \qquad where, f_d = \frac{f_{0j}}{f_{0i}} \qquad (13)$$

Figure 5. Surface S is oriented at an angle $\phi = \alpha$. Two points I and J, selected on the image plane correspond to points P_i and P_j on the surface. The viewing axis intersects the surface at P_0, with depth Z_0. The image plane is orthogonal to the view direction, and is viewed in the figure as a line.

It is necessary to identify a pair of points on the image plane which are projections of a pair of points, say P_1 and P_2, on S. Once this is done, K may be computed from the corresponding spectral values, f_{o1} and f_{o2}, at the projections of P_1 and P_2 on the image plane.

Next we discuss, how K is used to obtain the surface orientation. From Figure 5 select two appropriate points on the vertical axis on the image plane, with coordinates (x_i, y_i) and (x_i, y_j) (algorithm for the selection of this pair of appropriate points, is discussed later on in this section). These may be considered to be the projections of points P_i and P_j on the surface S.

From figure 5, using similarity of triangles we can write:

$$\frac{\Delta y_{ij}}{F} = \frac{\Delta Y_{ij} - \Delta Z_{ij}(\tan\gamma)}{Z_0 - \frac{\Delta Z_{ij}}{2}} \qquad (14)$$

where, $\tan(\gamma) = y_j/F$, $\Delta y_{ij} = y_j - y_i$ and $\Delta Y_{ij} = Y_j - Y_i$.
From equation (14) we obtain (see Appendix):

$$\cot\alpha = \frac{(2-K)\Delta y_{ij}}{2KF} + \tan\gamma$$

$$let, C_y = \frac{(2-K)\Delta y_{ij}}{2KF} + \tan\gamma$$

Then the expression of the azimuthal angle is:

$$\phi = \alpha = \arctan(1/C_y) \qquad if\ C_y\ is\ +ve$$
$$= \pi - \arctan(1/C_y) \qquad if\ C_y\ is\ -ve \qquad (15)$$

Similarly the polar angle θ is:

$$\theta = \arctan(1/C_x) \quad \text{if } C_x \text{ is } +ve$$
$$= \pi - \arctan(1/C_x) \quad \text{if } C_x \text{ is } -ve \qquad (16)$$

$$where, C_x = \frac{(2-K)\Delta x_{ij}}{2KF} + x_j / F$$

For determining the value of K, we need to choose a suitable pair of points on any one of the orthogonal axis of the image plane (vertical axis for obtaining α, horizontal axis for obtaining β). Let us consider the case of the vertical axis (obtain the value α). We need to identify a pair of points (x_1, y_1) and (x_1, y_2), with spectral frequencies f_{o1} and f_{o2}, which satisfy equation (12). The frequency at coordinate $(x_1,0)$ is f_{rp}. The steps are as follows:

a) First, select a point (x_1, y_1) $(y_1 <> 0)$ and observe its frequency f_{o1}.
b) Observe the frequency f_{rp} at coordinates $(x_1,0)$.
c) Search for y_k ($y_k > 0$ if y_1 is –ve,
    else < 0 if y_1 is +ve)
    and select $y_2 = y_k$, where $f_{o2} = f_{ok} = (2 f_{rp} - f_{o1})$

K is computed using equation (13), F is known from camera calibration, or may be considered to be unity, in which case the coordinates of the image plane must be scaled w.r.t. the focal length of the camera (focal length normalized image coordinates).

The advantage of the proposed method is the separable analysis in x and y directions which gives the polar and azimuth angles of the surface orientation respectively. The depth information (upto a scale factor [9, 15], in the absence of any additional information) can also retrieved using the analytical expressions derived (see equations (8) - (11)). In the next section, we illustrate the advantage of using wavelet transform in detecting spectral differences in texture images with experimentation on simulated data.

4. Wavelet based texture analysis and results

Let us consider two 1-D signals obtained by scanning along the horizontal lines of two texture images, of the same texture surface with difference in one of the angles of orientation. The images (see figure 6) are simulated as a superimposition of two simple sinusoidal patterns. Typical plots (signal I and signal II) of the horizontal scan lines of the pair of images in figure 6, are shown in figure 7. The corresponding spectral plots are shown in figure 8. Most spectral based methods [14, 18, 19] involves locating and finding the difference in the local spectral peaks of the signals. This process if often erroneous and difficult even for simple signals as shown in figure 8 (note that there are two separate and almost identical peaks in each plot). Hence it is necessary to use a multi-rate and multi-resolution filter bank to discriminate these features, rather than the use of a simple Fourier based analysis.

We suggest the use of wavelet transform for this purpose. The plot of the wavelet coefficients for the pair of signals in figure 7, are shown in figure 9 (detail coefficients at level 1, i.e. D1, are negligible and are hence not illustrated). Daubechies 6-tap dyadic filters [5] with 3 levels of decomposition are used for this purpose. The wavelet features exhibit a distinct difference in the response noticeably at detail levels 2 and 3 (compare the responses among the pairs of plots in figures 8 and 9). The process of
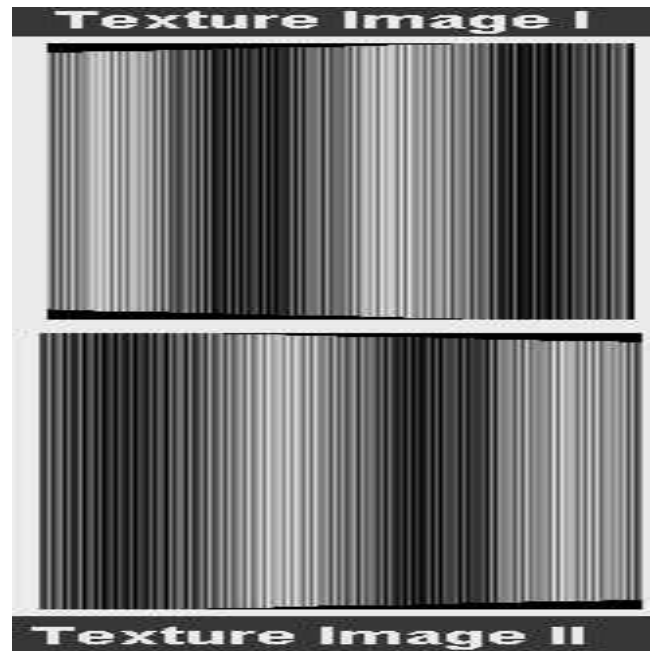

Figure 6. Two simulated texture images of the same surface with a difference in the orientation angle (ϕ=0 in both, θ = -42 deg. for Image I and 40 deg. for Image II).
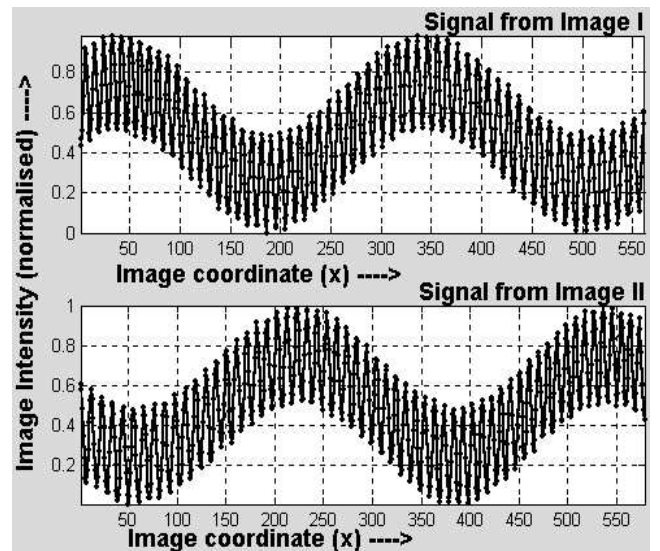

Figure 7. Two horizontal intensity profiles of the pair of images shown in figure 6 respectively.
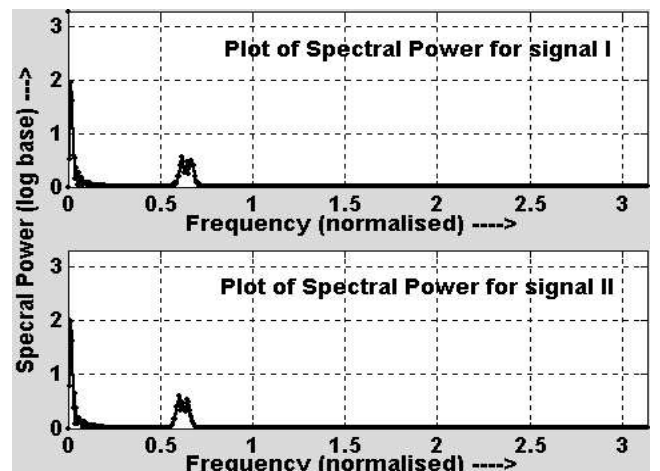

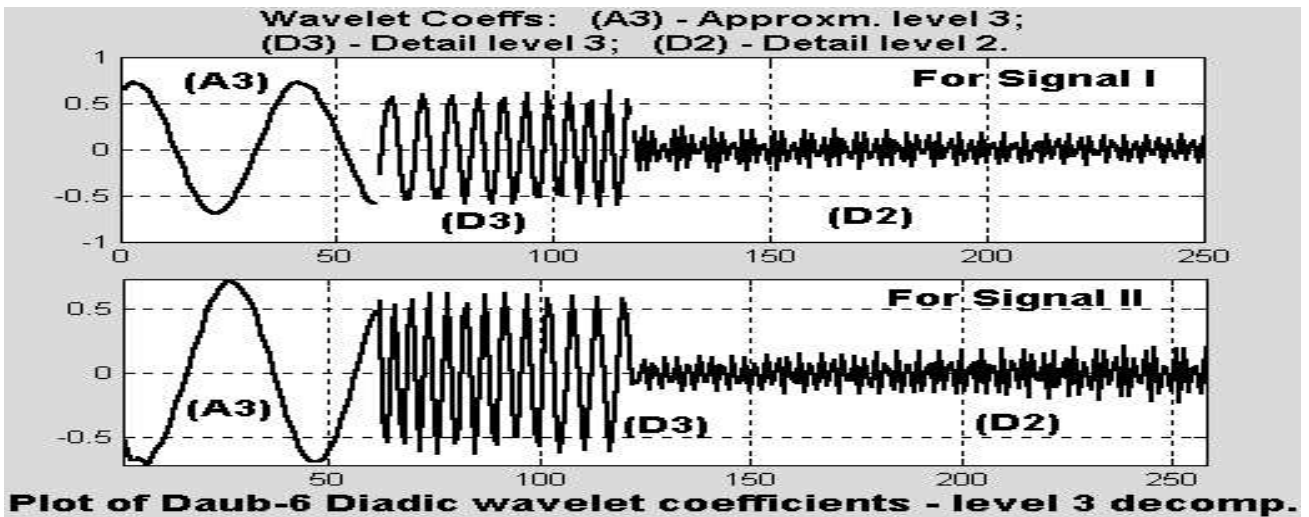Figure 8. Plots of spectral power for the pair of 1-D intensity profiles shown in figure 7 respectively.

Figure 9. Plots of the wavelet coefficients (level 3 decomposition) of the signals shown in figure 7 respectively.
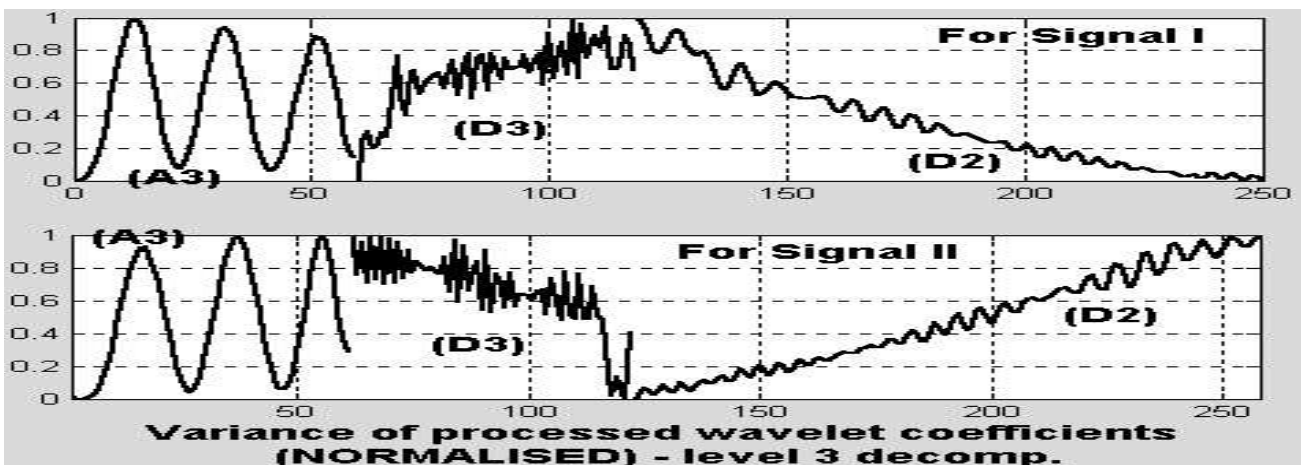

Figure 10. Features of the signals at the corresponding levels derived from the wavelet coefficients (in figure 9).

feature extraction from the wavelet coefficients consists of two steps. The first step of processing involves mean subtraction, squaring and Gaussian smoothing. The second step involves computing the variances of the post-processed signals, for each level of decomposition (namely, A3, D3 and D2) separately. Plots of the variance of the post-processed signals are illustrated in figure 10, which are derived from the wavelet coefficients shown in figure 9.

A weighted (obtained empirically) sum of the differences of the variances of the post-processed coefficients in the corresponding bands of the wavelet decomposition is related to the orientation angle and depth of the surface, as illustrated in figure 4. A ratio of these weighted sums computed at the pair of points P_1 and P_2, gives the value of f_d which is used to compute K as in equation (13).

Normalized observed frequencies, (f_{oi}/f_r), are computed using the proposed method for seven different orientations of the texture surface, with the simulated texture pattern as in figure 6. The actual and estimated values of the normalized observed frequencies are shown in figure 11. Discussions on accuracy and experimentation with real world data are beyond the scope of this current paper.

5. Conclusion
This paper illustrates the advantage of using wavelet transform to extract the orientation (in 3-D) of a textured planar surface. It promises to be powerful than the spectral based methods used in [1, 2, 6, 10, 11, 14, 16, 18, 19]. The weighted sum of the differences of the variances of the post-processed wavelet coefficients in the respective bands, is used to obtain the orientation of the texture surface. Expressions relating the orientation and depth of a texture surface with the spectral contents of the image texture have been derived. The method will be helpful in cases where the spectral characteristics of a texture (f_r) is known.

The proposed method has some drawbacks. It is assumed that surface S intersects the X-Z plane of the world coordinate system. This is necessary for detecting a pair of points in the image plane which satisfy equations (11-12). Errors in estimation are high when any of the angles of orientation of the surface and image resolution are small. Results are shown using superimposed sinusoidal signals to illustrate the effectiveness and utility of the proposed method.

Appendix
From equation (14)

$$\frac{\Delta y_{ij}}{F} = \frac{\Delta Y_{ij} - \Delta Z_{ij}(\tan \gamma)}{Z_0 - \frac{\Delta Z_{ij}}{2}} \qquad (A.1)$$
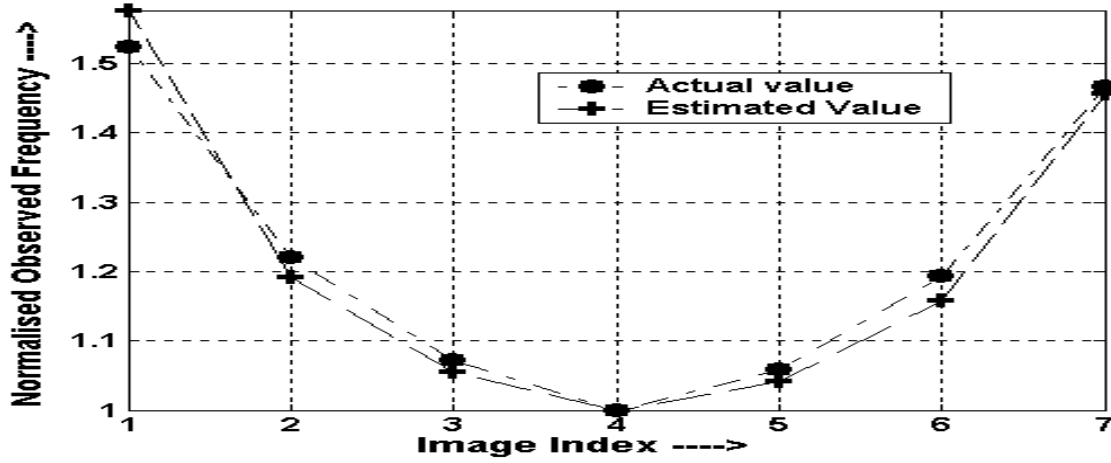
Figure 11. Actual and estimated values of the normalised observed frequncy for a set of seven images of the simulated texture pattern, with orientation angles ($\phi = 0$ in all cases) θ = -49, -35, -21, 0, 19, 33 and 47 degrees respectively. Estimation is based on the feature derived from detail level 2 (i.e. D2) coefficients only.

Since $\dfrac{\Delta Z_{ij}}{\Delta Y_{ij}} = \tan\alpha$, from (A.1), we have:

$$\frac{\Delta y_{ij}}{F} = \frac{2(\Delta Z_{ij})(\cot\alpha - \tan\gamma)}{2Z_0 - \Delta Z_{ij}}$$

Thus, $\cot\alpha = \dfrac{(2Z_0 - \Delta Z_{ij})\Delta y_{ij}}{2F(\Delta Z_{ij})} + \tan\gamma$

$$= \frac{(2-K)\Delta y_{12}}{2KF} + \tan\gamma$$

References

[1] P. N. Belhumeur and A. L. Yuille, Recovering Object Surfaces from Viewed changes in Surface Texture Patterns, Proceedings of the IEEE Conference on Computer Vision (ICCV '95), 1995, pp 876-881.

[2] Y. Choe and R. L. Kashyap, 3-D shape from a shaded and textural surface image, IEEE Transactions on Pattern Analysis and Machine Intelligence, Vol. 13, No. 9, September 1991, pp. 907-919.

[3] M. Clerc and S. Mallat, The Texture Gradient Equation for Recovering Shape from Texture, IEEE Transactions on Pattern Analysis and Machine Intelligence, Vol. 24, No. 4, April 2002, pp 536-549.

[4] K. J. Dana, Shree K Nayar, B. V. Ginneken and J. J. Koenderink, Reflectance and texture of real-world surfaces, Proc. IEEE-CVPR, June 1997, pp 151-157.

[5] I. Daubechies, Wavelets, Philadelphia, Pa.: S.I.A.M, 1992.

[6] J. Garding, Surface Orientation and Curvature from Differential Texture Distortion, Proceedings of the IEEE Conference on Computer Vision (ICCV '95), 1995, pp 733-739.

[7] B. K. P. Horn and M. J. Brooks, Shape from shading, MIT Press, 1989.

[8] V. Interrante, H. Fuchs and S. M. Pizer, Conveying the 3-D shape of smoothly curving Transparent Surfaces via Texture, IEEE Transactions on Visualization and Computer Graphics, Vol. 3, No. 2, April.June 1997, pp 98-117.

[9] Y. Jiang and H. Bunke, Dreidiemsionales Computersehen, Springer Verlag, 1997.

[10] J. S. Kwon, H. K. Hong and J. S Choi, Obtaining a 3-D orientation of Projective textures using a Morphological Method, Pattern Recognition, Vol. 29, 1996, pp 725-732.

[11] T. leung and J. Malik, On Perpendicular textures, or: Why do we see more flowers in the distance?, Proceedings of the IEEE Conference on Computer Vision and Pattern Recognition (CVPR '97), 1997, pp 807-813.

[12] S. K. Nayar, K. Ikeuchi and T. Kanade, Surface reflection: physical and geometric perspectives, IEEE Transactions on Pattern Analysis and Machine Intelligence, Vol. 13, No. 7, July 1991, pp 611-634.

[13] M. Oren and S. K.Nayar, Generalization of the Lambertian model and implications for machine vision, International journal of Computer Vision, Vol. 14, 1995, pp 227-251.

[14] E. Ribeiro and E. R. Hancock, Shape from periodic Texture using the eigenvectors of local affine distortion, IEEE Transactions on Pattern Analysis and Machine Intelligence, Vol. 23, No. 12, Dec. 2001, pp 1459 – 1465.

[15] Y. Shirai, Three-dimensional Computer Vision, Springer-Verlag, 1987.

[16] J. V. Stone and S. D. Isard, Adaptive Scale Filtering: A general method for obtaining shape from Texture, IEEE Transactions on Pattern Analysis and Machine Intelligence, Vol. 17, No. 7, July 1995, pp 713-718.

[17] P. Suen and G. Healey, The analysis and recognition of real-world textures in three-dimensions, IEEE Transactions on Pattern Analysis and Machine Intelligence, Vol. 22, No. 5, May 2000, pp 491-503.

[18] B. J. Super and A. C. Bovik, Planar surface orientation from texture spatial frequencies, Pattern Recognition, Vol. 28, No. 5, 1995, pp 729-743.

[19] B. J. Super and A. C. Bovik, Shape from Texture using local spectral moments, IEEE Transactions on Pattern Analysis and Machine Intelligence, Vol. 17, No. 4, April 1995, pp 333-343.